Analyst

Real-time imaging of cancer cell chemotaxis in paper-based scaffolds

Journal:	*Analyst*
Manuscript ID	AN-ART-09-2015-001787.R1
Article Type:	Paper
Date Submitted by the Author:	22-Oct-2015
Complete List of Authors:	Kenney, Rachael; University of North Carolina at Chapel Hill, Chemistry Boyce, Matthew; University of North Carolina at Chapel Hill, Chemistry Truong, Andrew; University of North Carolina at Chapel Hill, Chemistry Bagnell, C.; The University of North Carolina at Chapel Hill, Pathology and Laboratory Medicine Lockett, Matthew; The University of North Carolina at Chapel Hill, Chemistry

Real-time imaging of cancer cell chemotaxis in paper-based scaffolds

Rachael M. Kenney,[a] Matthew W. Boyce,[a] Andrew S. Truong,[a] C. Robert Bagnell,[b] Matthew R. Lockett[a,c]*

[a] Department of Chemistry, University of North Carolina at Chapel Hill, Kenan and Caudill Laboratories, 125 South Road, Chapel Hill, NC, 27599-3290

[b] Microscopy Services Laboratory, Pathology and Laboratory Medicine, University of North Carolina at Chapel Hill, 101 Manning Drive, Chapel Hill, NC 27599-7525

[c] Lineberger Comprehensive Cancer Center, University of North Carolina at Chapel Hill, 450 West Drive, Chapel Hill, NC 27599-7295

* Author to whom correspondence should be addressed: mlockett@unc.edu

Abstract

Cellular migration is the movement of cells, cultured as a monolayer; cellular invasion is similar to migration, but requires the cells to move through a three-dimensional material such as basement membrane extract or a synthetic hydrogel. Migration assays, such as the transwell assay, are widely used to study cellular movement because they are amenable to high-throughput screens with minimal experimental setup. These assays offer limited information about cellular responses to gradients *in vivo* because they oversimplify the three dimensional (3D) environment of a tissue. There are a number of invasion assays that support 3D cultures, some of which provide experimental control over the spatial and temporal gradients imparted on the culture. These assays, in their current form, are difficult to setup and maintain, and often require specialized laboratory equipment or engineering expertise. Here we describe a paper-based invasion assay in which cellular movement can be monitored in real-time with fluorescence microscopy. These assays are easily prepared and utilize materials commonly found in any laboratory: a single sheet of paper. These sheets are wax patterned to contain channels in which cells suspended in a hydrogel are seeded and cultured. Cell-containing sheets of paper are placed in a custom-built holder that allows gradients to form along the length of the channels. In this work, we compare the invasion of cells cultured in the presence and absence of an oxygen gradient. Our result support previous findings that oxygen is a chemoattractant, and selectively directs cellular movement in a 3D culture environment.

Keywords

Invasion assay, hypoxia, fluorescence microscopy, breast cancer, paper

Introduction

Chemotaxis—the directed movement of cells exposed to a gradient of cytokines, growth factors, or other small molecules—plays an important role in driving the invasion, intravasation, extravasation, and colonization of tumorigenic cells.[1-4] The steepness and shape of these gradients *in vivo* largely depend on the source of the chemotactic molecules and the concentration changes imposed by the surrounding matrix through adsorption, binding, and degradation of the molecules. There are a number of chemotaxis assays that screen for potential chemotactic molecules;[3, 5] these assays range in complexity from monolayer cultures to three-dimensional tissue-like structures.

Transwell assays are widely used to study chemotaxis because they are readily assembled, easy to analyze, and amenable to high-throughput screens.[5, 6] These assays provide an end-point readout, and enumerate cells that have migrated across a porous filter in the presence of an ill-defined gradient of a soluble factor. The monolayer cultures used in these assays oversimplify the environment of a tissue, and cannot readily mimic the cell-cell and cell-matrix interactions found *in vivo*. Microfluidic devices support two- and three-dimensional cultures, and offer exquisite control over the spatial and temporal gradients of soluble molecules delivered to the culture.[7, 8] Many of these devices are optically transparent and compatible with real-time imaging. Analysis of sequentially captured images makes it possible to distinguish chemotaxis from chemokinesis: the promotion of randomized migration.[4] Microfluidic devices have not been widely adopted by tissue culture laboratories because they, in their current state of development, are difficult to setup and maintain, requiring specialized equipment and engineering experience.[5]

There is a need for a culture system that provides: i) a three-dimensional culture environment, similar to *in vivo* conditions; ii) the ability to experimentally control the cellular environment through the formation and modulation of chemical gradients, akin to microfluidic devices; and iii) the ease of setup and analysis offered by migration assays, such as the transwell assay. Paper-based scaffolds are an attractive material for generating three-dimensional tissue-like structures because they can be prepared with equipment commonly found in a tissue culture laboratory. Whitesides and colleagues demonstrated that a culture of mammalian cells suspended

in a hydrogel could be maintained in wax-patterned sheets of paper for prolonged periods.[9-12] Paper-based devices are also ideal for studying chemotaxis of cells in static gradients because paper readily wicks liquids and has been used to fabricate low-cost microfluidic and flow-based devices.[13-15] Strips of paper containing static gradients of two chemokines were used to promote the chemotaxis of T lymphocytes; the chemokine-containing papers were placed atop cells cultured on fibronectin-coated surfaces.[16]

Paper-based scaffolds were recently adapted to study the invasion of non-small cell lung cancer cells in the presence of an oxygen gradient.[17] These "invasion stacks" were prepared by sandwiching wax-patterned sheets of paper containing cells suspended in a hydrogel between sheets of paper containing only hydrogel. The stacks were incubated in a custom-made holder that controlled the exchange of fresh medium with the culture, and generated a diffusion-dominated environment similar those established in solid tumors. During culture, cells invaded neighboring layers of hydrogel-containing paper; the individual sheets of paper were separated, and the extent and directionality of invasion in the applied gradient quantified. While these paper-based invasion assays are easily assembled and can be analyzed with fluorescence imaging techniques, they can only accommodate end-point analyses, as the stack must be disassembled prior to imaging.

Here, we describe a paper-based invasion assay that utilizes a single sheet of paper, which was patterned to contain three 11-millimeter long channels. This single-sheet format affords a three-dimensional culture environment in which cells can be directly imaged, in real-time, with fluorescence microscopy. This feature eliminates the need of disassembling the invasion assay prior to analysis. We monitored the invasion of breast adenocarcinoma (MDA-MB-231) cells in the presence and absence of an oxygen gradient. A prevailing hypothesis in tumor biology is that hypoxia promotes an invasive phenotype in cancer cells.[18-20] These hypoxic regions result in solid tumors because the oxygen demands of the highly proliferative cells outpace the supply provided by poorly formed and often aberrant vasculature;[21] this disparity of supply and demand results in oxygen gradients, which are believed to direct the movement of the invasive cells to neighboring tissues.

We found that MDA-MB-231 cells cultured in the single-sheet invasion assay selectively invade regions of higher oxygen concentration. To confirm the oxygen gradients were responsible for the observed chemotactic response, we performed control experiments and quantified cellular invasion in the absence of an oxygen

gradient. We also confirmed that cells, at increased distances from the source of oxygen in the channel, have increasing amounts of hypoxia inducible factor-1α (HIF-1α) localized in their nuclei. HIF-1α is a transcription factor whose localization in the nucleus is a hallmark of cells experiencing hypoxia. These experiments support the previous findings in the paper-based invasion stacks, and show that oxygen is a chemoattractant for more than one type of cancer cells. This work further demonstrates the ease in which paper-based cultures can be assembled to study cellular invasion, which can be monitored *in situ* over prolonged periods of incubation.

Experimental

Cells and culture reagents

We engineered MDA-MB-231 cells to constitutively express green fluorescent protein (M231-eGFP) using lentiviral particles purchased from GeneCopoeia (LPP-eGFP-Lv105-025). This cell line was transduced according to the manufacturer's protocol and maintained with puromycin (1 μg/mL). Parental and M231-eGFP cells were cultured in vented tissue flasks at 37 ^{o}C and 5% CO_2 in RPMI 1640 medium (Gibco, Life Technologies) containing fetal bovine serum (10% v/v) and penicillin-streptomycin (1% v/v). Culture medium was exchanged every two days. These cells were passed when the culture reached 70 – 80% confluency: the cells were detached from a tissue culture flask with Trypsin-EDTA (5 minutes, 37^{o}C), washed with serum-containing medium, pelleted, and cultured in a fresh flask at the appropriate dilution.

Paper-based scaffold preparation

We prepared the paper-based scaffolds (Figure 1A) by patterning Whatman 105 lens paper with wax from a Xerox ColorCube 8870 printer. Each pattern contained three 11.0 mm x 2.5 mm channels. Each scaffold was patterned with black-colored wax, which is not fluorescent, allowing cell-containing regions to be easily distinguished from the wax background. The scaffolds also contained a series of red-colored wax lines; these lines helped with setup and analysis because they are readily visualized by eye and are fluorescent. These

patterns are detailed in Figure S1 of the SI. Each scaffold was baked at 150 ^{o}C for 15 minutes to ensure the wax completely permeated the sheet, and was sterilized with ultraviolet light prior to use.

Sheets of cellulose acetate (overhead transparency films, Staples) were cut into defined designs with a Silver Bullet® cutting machine. The designs of the cellulose acetate films are detailed in Figure S2 of the SI. The cellulose acetate sheets were rinsed in 70% ethanol and autoclaved prior to use. Polydimethylsiloxane (PDMS) films were prepared by spin coating a mixture of Sylgard® 184 silicone elastomer curing agent and base (1:10 ratio, Dow Corning) onto a cellulose acetate film with the following protocol: step 1, speed (S) = 4 sec at 300 rpm, and acceleration (A) = 278 rpm/sec; step 2, S = 30 sec at 400 rpm, A = 417 rpm/sec. A sheet of Whatman 105 paper was placed atop the PDMS film prior to curing overnight at 150 ^{o}C. The 100 μm thick PDMS films were cut into defined designs with a Silver Bullet® cutting tool, separated from the cellulose acetate films, and sterilized under ultraviolet light (30 minutes per side) prior to use. The designs of the PDMS films are detailed in Figure S2 of the SI.

Assembly of the single-sheet invasion assays

Prior to assembling the invasion assays, cells were detached from a tissue culture flask as described above, washed, and resuspended in Matrigel (Corning) to a final concentration of 150,000 cells/μL; the Matrigel and cell suspension were kept on ice to prevent gelation. Cell-free Matrigel (0.59 μL) was added to 4-mm segments at the left and right side of the channel (Figure 2A), and the remainder of the channel was seeded with 0.44 μL of the cell-containing suspension. After seeding each of the channels, the paper-based scaffolds were placed in a six-well plate containing pre-warmed medium and incubated overnight (37 ^{o}C, 5% CO_2).

We utilized two culture setups. In one setup, the paper-based scaffold was sandwiched between two cellulose acetate films (Figure 1C). In the second setup, the paper-based scaffold was sandwiched between a cellulose acetate film and a thin film of PDMS (Figure 1D). Both setups, once assembled, were placed in a custom-made stainless steel holder and incubated for 48 h (37 ^{o}C, 5% CO_2). The culture medium was changed every 24 hours. The design of the stainless steel holder is detailed in Figure S3 of the SI.

Image acquisition and processing

Images of each channel were captured on an Olympus IX81 inverted light microscope equipped with a 4x/0.13 PhL UPlanFLN objective, an X-Cite lamp with a liquid light guide, and a 482 ± 17 nm emission filter. The six-well plates containing the stainless steel holders were placed on a fully motorized LEP Bioprecision stage, which was controlled by Improvision's Velocity Software. Each channel was captured as a series of six images, each with 10% overlap, that were digitally stitched together to form a single image.

Images were visualized and processed in ImageJ.[22] We used a custom-designed macro, which: aligned a series of sequential images (i.e., images of a particular channel after 0, 24, and 48 h of incubation) from a user-defined line running the length of the channel; determined the center of mass for defined regions of the channel; and compared these center of mass values to the first image in the series. The annotated code of the macro is provided in the SI.

Immunofluorescence

Samples were immediately fixed at the completion of the invasion assay to prevent protein degradation of hypoxia inducible factor-1 alpha (HIF-1α) upon reoxygenation.[23] The assembled invasion assays were quickly rinsed in 1X DPBS (Life Technologies), submerged in a solution of 4% formalin (Life Technologies) in 1X DPBS, and disassembled. The paper-based scaffolds were incubated in the formalin solution for 15 minutes, and permeabilized in wash buffer (1X PBS, 0.3% Triton X-100) for 1 hour at room temperature. The samples were blocked in wash buffer containing 5% normal goat serum (Cell Signaling Technology) for 1 hour at room temperature and then incubated overnight at 4 ^{o}C with mouse anti-HIF-1α-Dylight 550 (1:200 dilution; Life Technologies). The samples were washed four times with wash buffer and then incubated for 3 hours at room temperature in phalloidin-CruzFluor 633 (1:10,000 dilution, Santa Cruz Biotechnology) and DAPI (1:1,000 dilution, Life Technologies). The stained samples were washed six times with wash buffer and three times with 1X DPBS prior to mounting onto glass slides with Prolong® Gold Antifade Reagent (Cell Signaling Technology).

Images were obtained on a Zeiss LSM 700 confocal laser scanning microscope using a 20X/0.80 Plan-Apochromatic objective. Each image (1024 x 1024 pixels) was obtained at an acquisition speed of 1.58 µs/pix and is the average of four images.

Statistical analyses

Values presented in this work are the mean and standard deviation of at least five replicate invasion assays. A two-tailed Student's t-test was used to compare different sets of data; a p-value of < 0.05 was considered significant.

Results and Discussion

Single-sheet invasion assay fabrication.

We chose Whatman 105 lens paper to prepare the single-sheet invasion assay because it is thin (~35 µm thick) and has a low density of fibers (~80% void volume), allowing us to directly visualize cells in the paper-based scaffolds with a light or fluorescence microscope. Each wax-patterned scaffold (Figure 1A) contained three channels, and allowed us to perform three technical replicates in a single experimental setup. Suspensions of cells in Matrigel were seeded in the channel as depicted in Figure 2A. The scaffolds were sandwiched between two sheets of cellulose acetate and placed in a custom-made stainless steel holder (Figure 1B). We selected cellulose acetate because it is transparent, and allowed us to directly visualize the cells in the assembled holder with an inverted fluorescence microscope. These sheets are also impermeable to liquids and oxygen, allowing us to limit the exchange between the culture medium and the channel. Gradients generated in the channel result from diffusion-dominated mass transport and cellular consumption. Both the paper-based scaffolds and the cellulose acetate films are readily modified to generate gradients of different shapes or steepness, on an experiment-by-experiment basis.

Tracking Cellular Invasion.

We engineered MDA-MB-231 cells to constitutively express green fluorescent protein. We tracked the movement of these eGFP-expressing cells in the paper-based scaffolds with an inverted fluorescence

microscope, and collected images of each channel after 0, 24, and 48 hours of incubation. Images of each channel are composites stitched together from six individual images that cover the length of the channel. Unlike many chemotaxis assays, which utilize microscopy-based readouts to track the movement of a small number of individual cells (typically 20 or fewer),[24-27] we measured the average movement of all the cells in the invasion assay. To quantify the average displacement of the cells in the channel after 24 or 48 h of incubation, we designed a macro in ImageJ to locate the cell fronts at the left- and right-hand side of the cell-containing region. The macro automatically identifies both cell fronts, and draws a box extending from a pre-defined location (the 3.0 or 9.0 mm marking, Figure 2A) until the average fluorescence signal of the bulk cell population is reached. The macro determines the size and location of these boxes for the initial image (Figure 3A), calculates the center of mass of the cells at the start of the invasion assay, and then measures the center of mass for the same region of interest in the subsequently captured images.

Measuring the bulk movement of an entire population of cells distills invasion into a single value: the average distance traveled by a dense population of cells experiencing differing levels of oxygenation, nutrient starvation, and exposure to cellular waste products. Changes in center of mass for a given period of incubation allowed us to quantify the average movement of both cell fronts. This method of analysis is entirely independent of variations in image intensity and eliminates problems that could arise between image acquisitions, such as: slight differences in the plane of focus, inconsistent settings during image acquisition, or slight variations in the illuminated field. In the current work, we chose to focus on the cell fronts to demonstrate the feasibility of quantifying average cellular movement in the single-sheet invasion assays. The macro can be adapted to define multiple regions of interest, and is also capable of tracking the movement of smaller numbers of cells.

Cells selectively invade regions of higher oxygen concentration.

Previous work in paper-based invasion stacks[17] found that lung adenocarcinoma cells, when placed in an oxygen gradient, selectively invade regions of higher oxygen concentration. To determine if oxygen acts as a chemoattractant for other cell types we compared the movement of M231-eGFP cells in the presence and absence of an oxygen gradient. To generate monotonic gradients of oxygen and other soluble factors along the

length of the channel, we used the setup shown in Figure 1C and measured the movement of the cell fronts with the macro described above. The cell front closest to the region of free exchange with the culture medium is referred to as the "proximal cell front"; the "distal cell front" is further away from the region of exchange. Invasion toward the region of free exchange is indicated by positive values, while movement away is indicated by negative values.[28]

When assembling the invasion assays, we placed the M231-eGFP cells in two different locations in the channel, such that the proximal cell front was either 0.5 or 1.0 mm from the region where medium freely exchanged with the culture. For channels under an oxygen gradient, cell placement had a significant affect on the movement of the cells toward regions of higher oxygen concentration (Figure 3). Cells seeded 1.0 mm away from the opening did not undergo chemotaxis after 24 h of incubation, and the change in center mass for the proximal and distal cells fronts is not statistically significant. After 48 h, cells at the proximal front migrated 73 ± 40 μm toward the region of free exchange while cells at the distal front migrated 24 ± 20 μm away from the oxygen source. These differences are statistically significantly greater ($p < 0.05$), and indicate the cells are preferentially invading toward regions of higher oxygen concentration.

The proximal cell front of cells seeded 0.5 mm from the oxygen preferentially migrated toward the oxygen source at 24 h ($p < 0.001$) and 48 h ($p < 0.005$). The observed difference in cell invasion can be attributed to placement of the cells in the oxygen gradient. Cells have been shown to be sensitive to the steepness of the oxygen gradients, and increasing distances from the source of oxygen will result in a shallower gradient that is not as easily detected by the cells.[26] The shape of the oxygen gradient, which is a result of diffusion into the system and consumption by the cells, is greatly affected by the position and distribution of the cells seeded in the channel. This diffusion-consumption model of gradient formation provides a framework to better model the oxygen gradients formed in the paper-based cultures, and relies on technical improvements such as the reproducible seeding of cells in the channel.

To determine if the oxygen gradient, and no other changes in the cellular microenvironment such as decreased pH or the accumulation of signaling molecules or waste products, was responsible for the selective movement we observed, we repeated the above experiments with the setup shown in Figure 1D. Here, the top

cellulose acetate film was replaced with a 100 μm thick sheet of PDMS, which also contained a single opening to allow the exchange of fresh medium with the channel. This setup resulted in the formation of a monotonic gradient of soluble nutrients along the channel, but exposed the channel to a uniform concentration of oxygen. In these experiments the movement toward and away from the nutrient source after 24 and 48 h of culture are statistically insignificant, regardless of the location they were seeded in the channel (Figure 3).

Cells selectively express different levels of hypoxia inducible factor-1α in different locations of the oxygen gradient.

To further confirm that the directed movement of the M231-eGFP cells was caused by an oxygen gradient formed in the channel, we cultured parental MDA-MB-231 cells in various locations along the channel and immunofluorescently labeled them for HIF-1α. HIF-1α is constitutively expressed in all cells, and under normoxic conditions is rapidly hydroxylated and marked for degradation.[29-31] Under hypoxic conditions, HIF-1α is stabilized and translocates to the nucleus where it associates with other proteins to form an active transcription factor complex. This complex regulates the expression of more than 800 genes.[31]

We assembled invasion assays as described above, and cultured parental MDA-MB-231 cells for 48 h in the presence of absence of an oxygen gradient. We seeded the cells: i) at the opening where medium freely exchanges with the culture, the proximal location; ii) 1.0 mm away from the opening, an intermediate location; and iii) 5.0 mm away from the opening, a distal location. Each setup was disassembled in the presence of formalin to ensure the HIF-1α was not degraded when the sample was reoxygenated. The samples were stained with a fluorescently labeled anti-HIF-1α antibody, which we used to compare the relative levels of hypoxia each setup of cells was experiencing; fluorescently labeled phalloidin, which allowed us to localize each cell in the sample; and DAPI, which allowed us to localize the nucleus of each cell. To quantify the average amount of HIF-1α antibody in the nucleus of each cell, we used ImageJ to select each of the DAPI-stained nuclei as regions of interest. We then used those regions of interest to obtain the fluorescence intensity of HIF-1α. Figure 4 contains representative confocal images of a single viewing plane of cells cultured in the locations distal (Figure 4A) and proximal (Figure 4B) to the region of free exchange between the medium and the channel.

Figure 4C is a graphical representation of the average fluorescence intensity of each cell in the sample, and is the average of at least 46 individual cells. HIF-1α localization in the nucleus is statistically indistinguishable for cells cultured in different locations of the setup utilizing a PDMS film, and confirms that the entire channel is exposed to a uniform concentration of oxygen. There is a significant difference between HIF-1α localization in the nucleus for cells cultured in an oxygen gradient. Cells proximal to the culture medium contain a similar amount of HIF-1α as the cells cultured in uniform oxygen. When comparing the different locations along the channel, however, there is a significant difference in the amount of HIF-1α that localizes in the nucleus between the proximal and distal populations ($p < 0.005$).

These results confirmed that oxygen gradients are being formed in the single sheet invasion assays, and that the oxygen concentration decreases as you move down the channel, away from the oxygen source. It also confirms that the observed invasion is due to the applied oxygen gradient.

Conclusion

We describe a paper-based invasion assay that utilizes a single sheet of wax-patterned paper with three channels in which cells suspended in a hydrogel can be cultured. This paper-based scaffold provides a 3D culture environment that can be easily assembled using equipment found in a tissue culture laboratory. These scaffolds are also thin enough that the cells can be directly visualized in the assembled invasion assay with a light or fluorescence microscope. We utilized this system to study chemotaxis of MDA-MB-231 cells in gradients of oxygen. Through a series of control experiments, in which we monitored cellular movement in the absence of an oxygen gradient, we confirmed that oxygen is acting as a chemoattractant in the diffusion-dominated environment of the paper-based invasion assay.

While these paper-based cultures are more easily assembled and maintained than current microfluidic devices, the shape and steepness of the gradients formed in these paper-based assays is yet to be characterized. There is a need for experimental methods capable of measuring the distribution of oxygen in these 3D cultures. The experiments presented here demonstrate that the paper-based cultures can be utilized to study chemotaxis,

and through the aid of microscopic imaging can follow a single culture for a prolonged period of time without having to disassemble the culture.

Acknowledgements

This work was supported by start-up funds provided by the University of North Carolina. We would like to thank C. Chad Lloyd and Christian Lochbaum for helpful discussions and suggestions.

Supplementary Information

Electronic supplementary information (ESI) available: detailed schematics of the paper-based scaffolds, cellulose acetate films, and stainless steel holders; representative fluorescence micrographs of the invasion channels at different times of incubation; annotated code used to analyze the invasion data.

References

1. E. T. Roussos, J. S. Condeelis and A. Patsialou, *Nat. Rev. Cancer*, 2011, **11**, 573-587.
2. P. A. Iglesias and P. N. Devreotes, *Curr. Opin. Cell Biol.*, 2008, **20**, 35-40.
3. J. Wu, X. Wu and F. Lin, *Lab Chip*, 2013, **13**, 2484-2499.
4. R. J. Petrie, A. D. Doyle and K. M. Yamada, *Nat. Rev. Mol. Cell Biol.*, 2009, **10**, 538-549.
5. E. K. Sackmann, A. L. Fulton and D. J. Beebe, *Nature*, 2014, **507**, 181-189.
6. N. Kramer, A. Walzl, C. Unger, M. Rosner, G. Krupitza, M. Hengstschlager and H. Dolzing, *Mutat. Res., Rev. Mutat. Res.*, 2013, **752**, 10-24.
7. M. Mehling and S. Tay, *Curr. Opin. Biotechnol.*, 2014, **25**, 95-102.
8. D. Gao, H. X. Liu, Y. Y. Jiang and J. M. Lin, *TrAC, Trends Anal. Chem.*, 2012, **35**, 150-164.
9. F. Deiss, A. Mazzeo, E. Hong, D. E. Ingber, R. Derda and G. M. Whitesides, *Anal. Chem.*, 2013, **85**, 8085-8094.
10. R. Derda, A. Laromaine, A. Mammoto, S. K. Y. Tang, T. Mammoto, D. E. Ingber and G. M. Whitesides, *Proc. Natl. Acad. Sci., U.S.A.*, 2009, **106**, 18457-18462.
11. R. Derda, S. K. Y. Tang, A. Laromaine, B. Mosadegh, E. Hong, M. Mwangi, A. Mammoto, D. E. Ingber and G. M. Whitesides, *Plos One*, 2011, **6**, e18940.
12. B. Mosadegh, B. E. Dabiri, M. R. Lockett, R. Derda, P. Campbell, K. K. Parker and G. M. Whitesides, *Adv. Healthcare Mat.*, 2013, **3**, 1036-1043.
13. E. Carrilho, A. W. Martinez and G. M. Whitesides, *Anal. Chem.*, 2009, **81**, 7091-7095.
14. A. W. Martinez, S. T. Phillips, G. M. Whitesides and E. Carrilho, *Anal. Chem.*, 2010, **82**, 3-10.
15. A. K. Yetisen, M. S. Akram and C. R. Lowe, *Lab Chip*, 2013, **13**, 2210-2251.
16. D. I. Walsh, M. L. Lalli, J. M. Kassas, A. R. Asthagirl and S. K. Murthy, *Anal. Chem.*, 2015, **87**, 5505-5510.
17. B. Mosadegh, M. R. Lockett, K. T. Minn, K. A. Simon, K. Gilbert, S. Hillier, D. Newsome, H. Li, A. B. Hall, D. M. Boucher, B. K. Eustace and G. M. Whitesides, *Biomaterials*, 2015, **52**, 262-271.
18. V. Cristini, H. B. Frieboes, R. Gatenby, S. Caserta, M. Ferrari and J. Sinek, *Clin. Cancer Res.*, 2005, **11**, 6772-6779.
19. H. B. Frieboes, F. Jin, Y. L. Chuang, S. M. Wise, J. S. Lowengrub and V. Cristini, *J. Theor. Biol.*, 2010, **264**, 1254-1278.
20. R. Sullivan and C. H. Graham, *Cancer Metastasis Rev*, 2007, **26**, 319-331.
21. A. L. Harris, *Nat. Rev. Cancer*, 2002, **2**, 38-47.
22. Rasband, W.S. ImageJ, U.S. National Institutes of Health, Bethesda, Maryland, USA. imageJ.nih.gov/ij/.
23. G. D'Angelo, E. Duplan, B. Boyer, P. Vigne and C. Frelin, *J. Biol. Chem.*, 2003, **278**, 38183-38187.
24. B. Mosadegh, W. Saadi, S. J. Wang and N. L. Jeon, *Biotechnol. Bioeng.*, 2008, **100**, 1205-1213.
25. C.-W. Chang, Y.-J. Cheng, M. Tu, Y.-H. Chen, C.-C. Peng, W.-H. Liao and Y.-C. Tung, *Lab Chip*, 2014, **14**, 3762-3772.
26. S. J. Wang, W. Saadi, F. Lin, C. M. C. Nguyen and N. L. Jeon, *Exp. Cell Res.*, 2004, **300**, 180-189.
27. K. Funamoto, I. K. Zervantonakis, Y. C. Liu, C. J. Ochs, C. Kim and R. D. Kamm, *Lab Chip*, 2012, **12**, 4855-4863.

28. When conducting statistical analyses on the data, we compared the average movement toward and away from the oxygen source as positive values, and report p-values for those comparisons.
29. D. M. Gilkes, G. L. Semenza and D. Wirtz, *Nat. Rev. Cancer*, 2014, **14**, 430-439.
30. G. L. Semenza, *Trends Mol. Med.*, 2001, **7**, 345-350.
31. D. M. Gilkes and G. L. Semenza, *Future Oncol.*, 2013, **9**, 1623-1636.

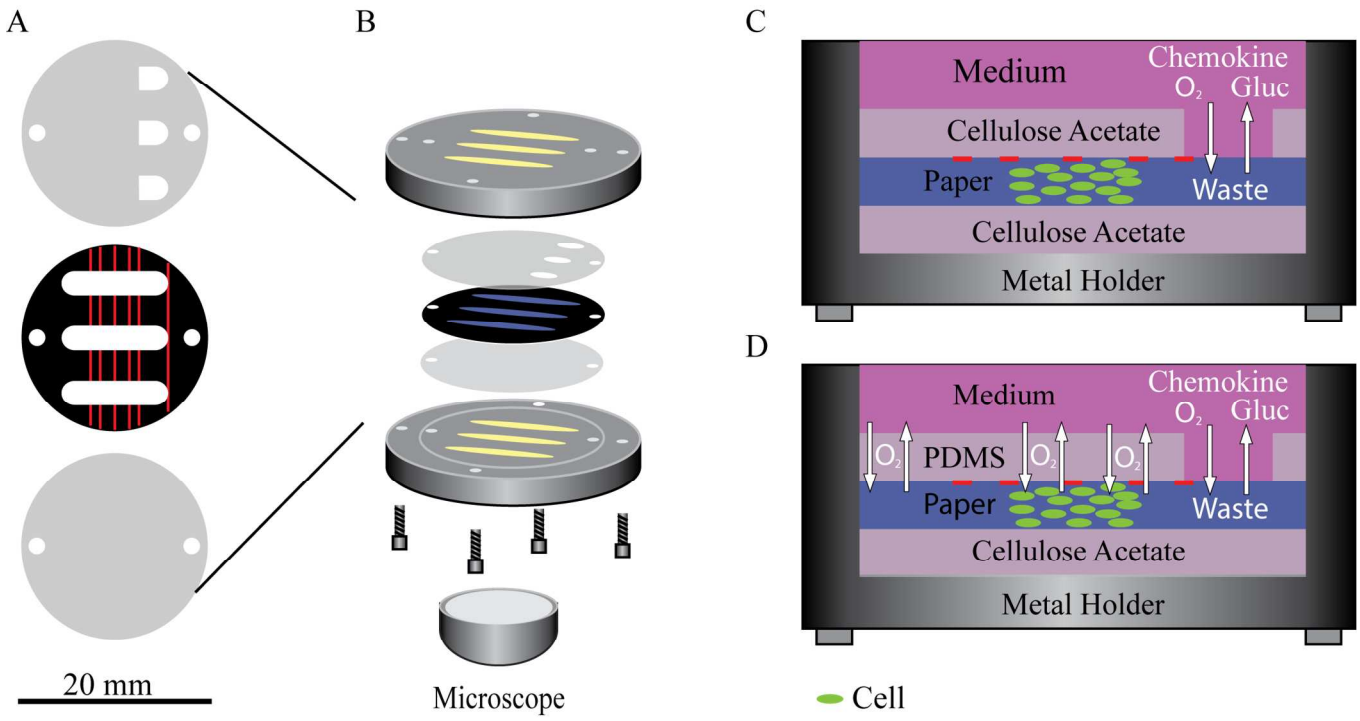

Figure 1. A) Schematic of a paper-based scaffold, patterned to contain three channels in which we cultured cells for the invasion assays. The scaffold is sandwiched between two cellulose acetate films. B) Schematic of an assembled invasion assay. The cell-containing scaffolds are assembled into a custom-made stainless steel holder. Cells in the assembled assay can be visualized directly with a light or fluorescence microscope. C) Side-view of an assembled invasion assay in which we use two cellulose acetate films to control the access of oxygen and other soluble nutrients to the culture. D) Side-view of an assembled invasion assay in which we replace the top cellulose acetate film with a thin sheet of PDMS. The PDMS limits the access of soluble nutrients to the culture but is freely permeable to oxygen. A) and B) are drawn to scale, as indicated by the scale bar in the lower left-hand corner of the figure. C) and D) are not drawn to the scale.

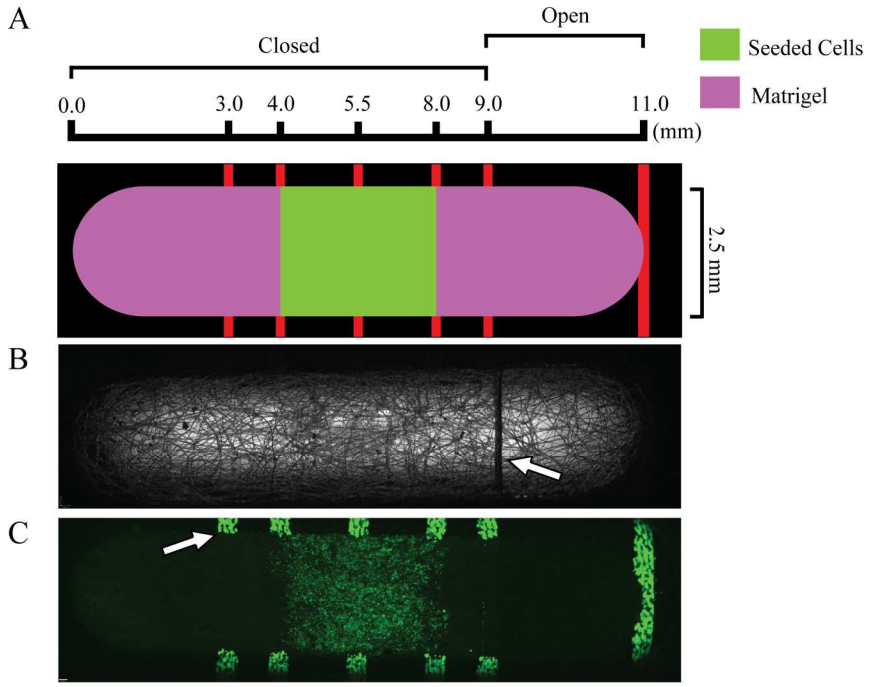

Figure 2. A) Schematic of the setup used for each invasion assay. Each channel is surrounded by black-colored wax and contains distance markers, which are red-colored wax. B) Bright field image of a single channel in the paper-based scaffold, the arrow white arrow denotes the edge of the top cellulose acetate film and the location in which medium was allowed to freely exchange with the culture. C) Fluorescence image of the same channel, seeded with M231-eGFP cells. The white arrow is pointing to one of the distance markers, which are fluorescent. The red-colored wax readily fluoresces and was used to visualize the position of the M231-eGFP cells in the channel and quantify bulk movement. The black-colored wax is not fluorescent.

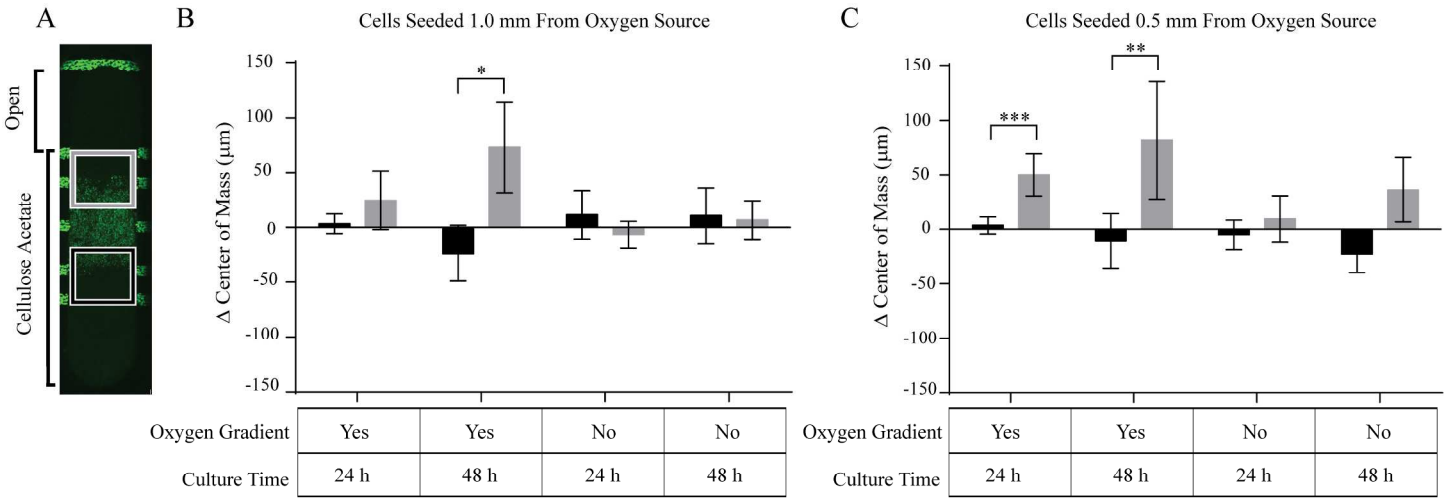

Figure 3. A) Representative fluorescence image of a channel with the distal and proximal regions of interest outlined by a black and gray box, respectively. These regions were selected by the macro detailed in the Supplementary Information section. Graphical representations of the average distance the cells moved is denoted as the change in center of mass for each experimental setup. Cells were seeded in the channel such that the proximal cell front was B) 1.0 or C) 0.5 mm away from the oxygen source. Each bar is the average of at least 5 replicates, and the error bars represent the standard deviation. A * represents $p < 0.05$; ** $p < 0.01$; *** $p < 0.001$; **** $p < 0.0001$.

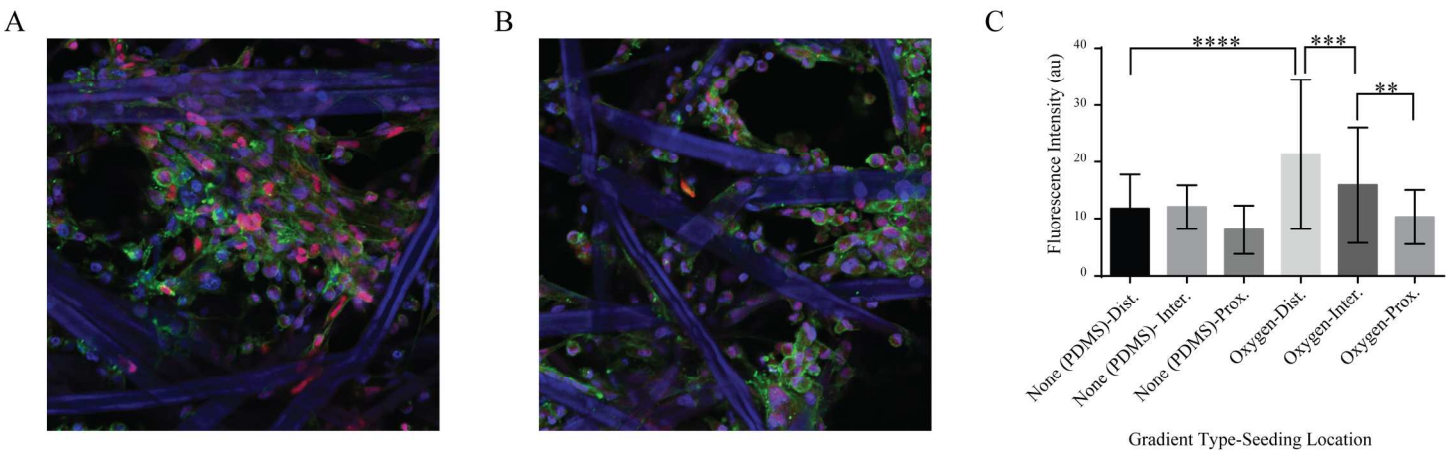

Figure 4. Representative immunofluorescence images of MDA-MB-231 cells in the paper-based channel stained for: HIF-1α staining (red), DAPI (blue), and phalloidin (green). Cells A) distal and B) proximal to the oxygen source were cultured for 48 h. We note that the fibers of the paper-based scaffolds were not selectively stained prior to imaging; these fibers fluoresce when excited with ultraviolet light, used to image the DAPI-stained nuclei. C) Graphical representation of the average fluorescence intensity of antibody-stained HIF-1α in the nuclei of cells cultured in various locations of the channel in the presence and absence of an oxygen gradient. Each bar is the average of at least n = 46 nuclei, and the error bars represent the standard deviation. A * represents $p < 0.05$; ** $p < 0.01$; *** $p < 0.001$; **** $p < 0.0001$.

TOC Figure:

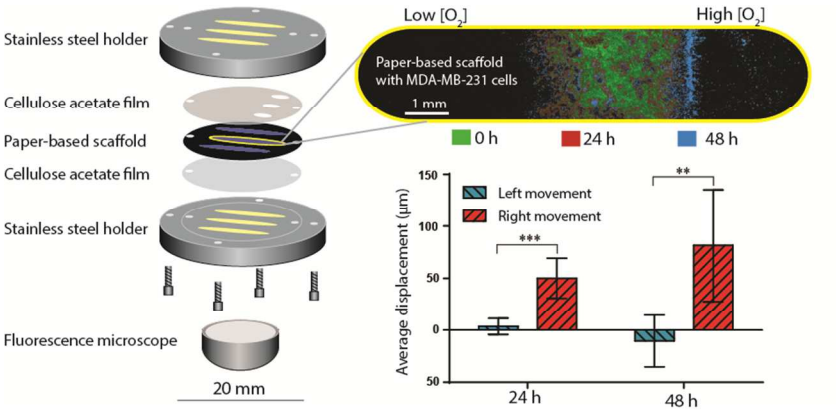

Statement:

An easy to assemble paper-based invasion assay to study chemotaxis of breast cancer cells in gradients of oxygen in real-time.